Contents lists available at ScienceDirect

Saudi Journal of Biological Sciences

journal homepage: www.sciencedirect.com

Original article

Influence of laser needle-knife on PI-3K, AKT and VEGF mRNA expression in cervical spondylotic arteriopathy model rabbits

Fang Liu [a,b], Lihong Ye [a,*], Wei Wei [a], Gaoyi Yang [a], Yang Ye [a], Jun Meng [a], Xueyan Din [b], Songjia Zhao [b]

[a] *Hangzhou Red Cross Hospital, Hangzhou 310003, China*
[b] *Zhejiang Chinese Medical University, Hangzhou 310053, China*

A B S T R A C T

Objective: To determine the effect of laser needle-knife on PI-3K, AKT and VEGF mRNA expression of vertebral arteries in a rabbit model of cervical spondylotic arteriopathy (CSA) and the mechanism of action involved.
Methods: Forty healthy general-grade rabbits were divided into a normal control group, model group, acupuncture group, and laser needle-knife group (n = 10 rabbits per group), and the CSA rabbit model was established in all but groups but the normal control group. CSA model rabbits in the acupuncture group were treated by acupuncture at the *Fengchi* (GB 20) and *Cervical Jiaji* (EX-B 2) points, whereas rabbits in the laser needle-knife group were treated with laser needle-knife targeting the *Jiaji* points near the C5 spinous process. Rabbits in the normal control and model groups were fixed using similar methods. Behavioral characteristics of all rabbits were evaluated before and after treatment. Peak systolic velocity (PSV) of the right carotid and vertebral arteries in each group were examined using beside B ultrasound, and PI-3K, AKT, VEGF mRNA expression in vertebral arteries were determined by real-time PCR.
Results: The behavioral signs of rabbits were improved after treatment in both the acupuncture and laser needle-knife groups. In comparison with control group, PSV of right carotid arteries in acupuncture group and laser needle-knife group were enhanced significantly (P < 0.05 and P < 0.01), PSV of right vertebral arteries in acupuncture group and laser needle-knife group were enhanced significantly too (P < 0.01 and P < 0.05). PI-3K mRNA expression in laser needle-knife and acupuncture group was significantly higher than that in control group (P < 0.01, P < 0.05). AKT mRNA expression in laser needle-knife and acupuncture group was significantly higher than that in control group (P < 0.01). VEGF mRNA expression in laser needle-knife and acupuncture group was significantly higher than that in control group too (P < 0.01, P < 0.05). No significant differences were found in PI-3K, AKT and VEGF mRNA expression levels among acupuncture and laser needle-knife groups (P > 0.05).
Conclusion: Laser needle-knife could effectively intervene the mRNA expression of PI-3K, AKT and VEGF, this may be one of the mechanisms of the effect of laser needle-knife in treating CSA in rabbits.

1. Introduction

Cervical spondylotic arteriopathy (CSA) involves a series of syndromes caused by the stimulation and compression of cervical nerve roots, spinal cord, vertebral arteries, and cervical sympa-

thetic nerves, and in traditional Chinese medicine, falls under the scope of dizziness and signs of stroke, according to Choi et al. (2014). There are many studies that have shown that the incidence of CSA is closely associated with steno-occlusive and circuitous shape of vertebral artery blood vessel (Kim, 2018; Zhu et al., 2018; Markus et al., 2018).

Acupuncture is one of the main traditional treatment for CSA, is widely used in clinical. But there are disadvantages such as time-consuming and have no lasting effect (Li et al., 2018; Hou et al., 2017; Wen et al., 2016; Deng et al., 2015). In order to research of rehabilitation medical value of laser-needleknife with supine repositioning massage therapy in CSA, 54 cases of CSA patients were treated by laser-needleknife combined with supine repositioning

* Corresponding author.
  E-mail address: bihaiyuxiao@126.com (L. Ye).
Peer review under responsibility of King Saud University.

Production and hosting by Elsevier

massage. Results from the finite element analysis indicated that the maximum flow rate of the left vertebral artery was improved by 47.52% in typical patients after the combined treatment while the surface force on vessels and the maximum shear force were reduced by 57.14% and 52.17% respectively (Liu et al., 2017). However, its mechanism is still controversial (Akin et al, 2017; Kevrekidis et al, 2018; Saranya et al, 2017).

Phosphatidylinositol 3-kinase (PI3K) is an intracellular signaling protein with catalytic activity. Activated PI3K phosphorylates protein kinase B (AKt) by binding to the latter's pH domains, and regulates cell proliferation and metabolism in mammals (Liu et al., 2015). Mammalian target of rapamycin (mTOR) is a downstream target of PI3K/AKt. AKt activates mTOR by phosphorylating the Ser-488 site of mTOR, which in turn increases the expression of a series of cell proliferation and differentiation-related proteins (Fu et al., 2018). In previous studies, it has been demonstrated that mTOR regulated the mRNA synthesis and protein expression of downstream hypoxia inducible factor (HIF) and promoted angiogenesis and local oxygen flow (Mao et al., 2018). Vascular endothelial growth factor (VEGF), which is more downstream of mTOR, is the most important angiogenesis-related factor among the 30+ factors that have currently been described (Chin et al., 2018). During hypoxia, HIF induced activation of VEGF transcription, which in turn increased capillary permeability and angiogenesis by promoting vascular endothelial cell division and proliferation (Chen et al., 2018).

In this study, we established a rabbit model of CSA by means of blood stasis and collateral obstruction and evaluated the efficacy of laser needle-knife in the treatment of CSA. We used scanning electron microscopy (SEM) to determine the effect of laser needle-knife on the micromorphological structure of the vertebral arteries in a CSA rabbit model and investigated alterations in the PI3K-AKt-VEGF signaling pathway as a possible therapeutic mechanism of this procedure.

2. Material and methods

2.1. Experimental animals

A total of 40 healthy general-grade adult rabbits (male and female in half) weighing 2.50 ± 0.2 kg were provided and housed in the Experimental Animal Center of Zhejiang Chinese Medical University.

2.2. Model construction

The rabbit model of CSA was established based on the methods described by Hu et al. (2005). In brief, blood was collected from the central ear artery of an allogeneic rabbit and mixed at a 1:1 ratio with 25% normal saline to prepare 9 mL of stagnant blood. Stagnant blood was injected into the right splenius cervicis, intramuscular and intermuscular gap of the intertransverse and transversospinalis muscles of the rabbits. Before and 2 weeks after the injection, all rabbits underwent color Doppler ultrasound imaging. Rabbits with >10 cm/s reduction in blood flow velocity in the right vertebral arteries were selected as model animals.

2.3. Grouping and treatment

40 rabbits were randomly divided into normal control group, model group, acupuncture group, and laser needle-knife group of 10 rabbits. CSA was induced in the acupuncture and laser needle-knife groups, but not in the normal control and model groups. Rabbits with failed CSA induction were removed from the groups at 2 weeks post-model construction.

Normal control group: CSA was not induced, and rabbits were fixed in a similar way as rabbits in the acupuncture group during treatment.

Model group: CSA was induced, and rabbits were fixed in a similar way as rabbits in the acupuncture group during treatment.

Acupuncture group: Treatment started at 2 weeks post-CSA induction. Acupuncture points: *Fengchi* point and *cervical Jiaji* points (C3-C7). Acupuncture method: #30 filiform needles (1.5 in.) were directly inserted into the above-mentioned 6 points using a twirling reinforcement-reduction method. Once the needles were in position, they were retained on the body for 30 min, appropriate adjustments were made every 10 min. Treatment was given once every two days for a total of 10 treatments. Rabbits were examined by color Doppler ultrasound on 20 d of treatment after which they were euthanized.

Laser needle-knife group: Treatment started at 2 weeks post-CSA induction. Procedures: (1) Position: rabbits were fixed in a surgical container in a prone position with cervical flexion. *Jiaji* points on both sides of the C5 spinous process, which can be found along the spinous process and vertebrae, were selected as the targets of treatment, and were based on the acupuncture point map of the experimental animal. (2) Skin disinfection: the skin of rabbits was disinfected using conventional iodophore. (3) Rabbits were locally anesthetized with 1% lidocaine. (4) The skin was cut, peeled, and loosened by laser needle-knife until no more nodules and blockage was felt. He-Ne laser radiation was applied to the needle at an output voltage of 200 mW in the beam expanding mode and on-off output. Treatment was 30 min in duration, and the site of treatment was covered by a Band-Aid after removal of the needle. The wound was kept dry for the next 24 h. Treatment was given once every 10 d for a total of 3 treatments. Rabbits underwent color Doppler ultrasound imaging on 20 d of treatment after with they were euthanized.

2.4. Main reagents and instruments

PSV of the right vertebral arteries of the rabbits was measured by portable bedside ultrasound (MICROMAXX, SonoSite Co., Ltd.); He-Ne laser therapy equipment (JH30C, Shanghai Jiading Optical Instrument, Co., Ltd., Shanghai, China), acupotome (HZ series, Beijing Zhuoyue Huayou Medical Devices Co., Ltd., Beijing, China) and acupuncture needle (#0. 25 * 40 mm, Wujiang Jia Chen Acupuncture Devices Co., Ltd., Wujiang, China) were used in treatment of CSA; Morphologies of the vertebral arteries of rabbits were examined with a scanning electron microscope (SU1510, Hitachi); RNA fast extraction kits (GK3016, Generay); HiScript- II Q RT SuperMix for qPCR (R222-01, Vazyme); ChamQ SYBR Color qPCR Master Mix (Q411-02, Vazyme); CFX connect Real-Time PCR System; The design, synthesis and purification of primers were provided with Shanghai Sonny Biotechnology Co., Ltd.

2.5. Behavior and signs

The spirit and manner (eyelid and physical movements), fur luster, nose and tail color, feces, hunching, and feeding behavior of all rabbits were observed daily and recorded once every 3 d starting from the day of CSA induction.

2.6. SEM

Rabbits in each group were euthanized by air embolism 2 days after completion of treatment. In brief, rabbits were disinfected, fixed, washed with boiling water, shaved, and relevant tissues were harvested for examination. The effect of treatment on the morphological structure of vertebral arteries in CSA rabbits was determined using SEM.

(1) Blood collection

Rabbits were euthanized and vertebral arteries and capillaries at the C4/5 and C5/6 joints were harvested under sterile conditions. Blood vessels were harvested and collected into culture dishes and washed with Hank's buffer. The adventitia was gently stripped using ophthalmic scissors and forceps.

(2) Preparation of decellularized matrix

The 1% TritonX-100 + 1% SDS method: (1) Blood vessels were washed 3 times with PBS and placed into 50 mL centrifuge tubes containing distilled water. Tubes were placed on a shaker (30 r/min) at 4 °C for 12 h for decolorization. (2) Blood vessels were transferred to centrifuge tubes containing 1% TritonX-100, and were placed on a shaker (30 r/min) at 4 °C for 24 h for decolorization, followed by 3 washes with PBS. (3) Distilled water was added to the tubes, and decolorization was continued at 4 °C for 4 h on the shaker (30 r/min). 4) Blood vessels were transferred to tubes containing 1% SDS, and were placed on a shaker (30 r/min) at 4 °C for 4 h for decolorization, followed by 3 washes with PBS. Next, distilled water was added to the tubes, and decolorization was continued under shaking (30 r/min) for 4 h. Fresh distilled water was replaced every 6 h for a total of 72 h of washing. Samples were frozen for future use.

(3) Preparation of SEM samples

Samples were mounted on copper stubs using conductive double-sided tape, sprayed with a layer of gold coating under vacuum conditions, and evaluated using a SU1510 scanning electron microscope (HITACHI).

2.7. Blood flow status of vertebral artery

The PSV of right carotid artery vertebral artery was determined by portable bedside ultrasound (frequency:13 MHz) before and 20 d after treatment.

2.8. mRNA expression

The total RNA was extracted by Trizol- centrifuge column method. Experimental parameters: 95.0 °C for 30 s, 95.0 °C for 10 s, 60.0 °C for 30 s Plate Read, GOTO 2, 40 reps, Melt Curve 70 °C to 95 °C : Increment 0.5 °C for 5 s Plate Read. PI3K, Akt, VEGF mRNA levels in rabbit vertebral arteries were determined according to the manufacturer's instructions.

2.9. Statistical analysis

Data were organized into an experimental result database and statistically analyzed using SPSS version 17.0 software (SPSS, Chicago, IL, USA). Data were expressed as the mean ± standard deviation (±s). $P < 0.01$ or $P < 0.05$ was considered statistically significant.

3. Results

3.1. General condition and behavior of rabbits

Prior to CSA induction, no significant differences were observed in the spirit and manner (eyelid and physical movements), fur luster, nose and tail color, feces, hunching, and feeding behavior between rabbits in each group. Model construction was relatively successful as no deaths were observed in the 30 model rabbits. Upon CSA induction, model rabbits gradually exhibited varying levels of spiritlessness, hunching, loss of appetite, lethargy and reduced activity, or delayed responsiveness that exacerbated over time. These symptoms were most apparent in the model group. In contrast, no significant changes were observed in the general condition of rabbits in the normal control group throughout the study. After treatment, different levels of improvements were observed in the general conditions of rabbits in the acupuncture and laser needle-knife groups. Specifically, reduced activity levels and spiritlessness were least observed in the acupuncture group, whereas hunching was least observed in the laser needle-knife group. These findings indicated that both acupuncture and laser needle-knife were effective in improving systemic and behavioral symptoms of CSA model rabbits.

3.2. SEM images of different samples

After completion of treatment, the surfaces of vertebral arteries of rabbits in each group were evaluated by SEM (Fig. 1).

In rabbits in the normal control group, as shown in Fig. 1-a, numerous folds were present on the surface of the decellularized matrix, indicating good nutrient and energy transport in vertebral arteries in the absence of CSA. Moreover, rabbits in the model group demonstrated more occluded arteries and fewer folds on the vascular surface, suggesting that CSA led to reduced blood and nutrient supply in vertebral arteries (Fig. 1-b). Upon treatment of rabbits in the acupuncture group (Fig. 1-c), a low level of capillary hyperplasia was observed on the vertebral artery surface, which improved microcirculation, increased blood flow volume and alleviated CSA symptoms. Similarly, treatment or rabbits in the laser needle-knife group resulted in greater capillary hyperplasia on the vertebral artery surface and an increased number of micropores on the surface and cross-sections of vertebral arteries (Fig. 1-d,e). Given that micropores are beneficial for the transport of nutrients, these findings suggested that the mechanism of action of laser needle-knife in the treatment of CSA may be associated with an increase in micropores (see Fig. 2).

3.3. Effect of laser needle-knife on blood flow of vertebral artery in CSA rabbits

Before the modeling, the right carotid artery and vertebral artery PSV of each rabbit group were statistically analyzed. There was no significant difference between the groups and they were comparable. 14 days after the model was established (before treatment), a rabbit with a decrease in the blood flow velocity of the right vertebral artery greater than 10 cm/s was selected as a successful model. The PSV of the right carotid artery and vertebral artery in the three groups of CSA rabbit models was significantly lower than that in the normal group ($P < 0.01$), and there was no significant difference between the three groups ($P > 0.05$). After 20 days of treatment, the PSV of the right carotid artery in the model group was significantly lower than that in the normal group ($P < 0.01$). There was no statistical significance in the right carotid artery PSV between the acupuncture group and the laser acupotomy group compared with the normal group ($P > 0.05$). Compared with the model group, the PSV of the carotid artery in the acupuncture group and the laser acupotomy group was significantly higher than that in the model group ($P < 0.05$, $P < 0.01$, respectively). After 20 days of treatment, the PSV of the right vertebral artery in the model group was significantly lower than that in the normal group ($P < 0.01$). There was no statistical significance in the right vertebral artery PSV between the acupuncture group and the laser acupotomy group compared with the normal group ($P > 0.05$). Compared with the model group, the PSV of the vertebral artery in the acupuncture group and the laser acupotomy group was significantly higher than that in the model group ($P < 0.05$, $P < 0.01$, respectively).
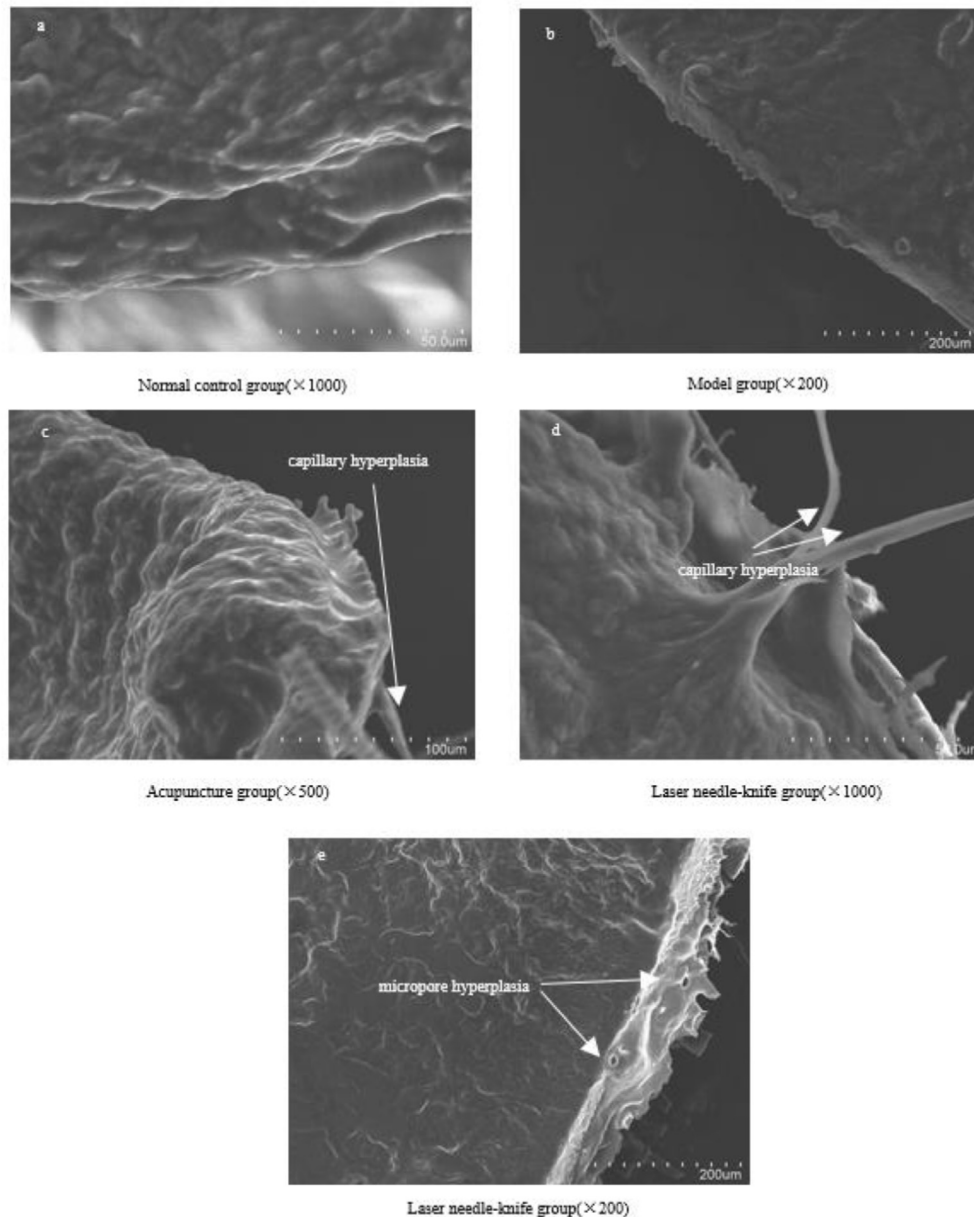
Fig. 1. SEM images of vertebral arteries of rabbits in each group.

3.4. Effect of laser needle-knife on levels of PI-3K, AKt, and VEGF mRNA expression in CSA rabbits

Post-treatment PI-3K mRNA expression levels in right cervical artery of rabbits per group are shown in Fig. 3. PI-3K mRNA expression levels were significantly lower in the model group compared to the normal control group ($P < 0.01$), but similar between acupuncture, laser needle-knife, and normal control groups ($P > 0.05$). In addition, PI-3K mRNA expression levels were significantly higher in the laser needle-knife and acupuncture groups compared to the model group ($P < 0.01$, $P < 0.05$), but was similar between the two treatment groups ($P > 0.05$).

Post-treatment p-AKt mRNA expression levels in the right cervical artery of rabbits per group are shown in Fig. 4. p-AKt mRNA concentration was significantly lower in the model group than in the normal control group ($P < 0.01$), but was similar between the acupuncture, laser needle-knife and normal control groups ($P > 0.05$). p-AKT mRNA concentration was significantly higher in

the acupuncture and laser needle-knife groups than in the model group (both $P < 0.01$), but was similar between the two treatment groups ($P > 0.05$).

Post-treatment VEGF mRNA levels in the right cervical artery of rabbits per group are shown in Fig. 5. The VEGF levels were significantly lower in the model group compared to the normal control group ($P < 0.05$), but were similar between acupuncture, laser needle-knife, and normal control groups ($P > 0.05$). Moreover, VEGF levels were significantly higher in the laser needle-knife and acupuncture groups compared to the model group ($P < 0.01$ and $P < 0.05$), but were similar between the two treatment groups ($P > 0.05$).

4. Discussion

PI-3K is a signal protein with intracellular catalytic activity, its activation results in the production of a second messenger PIP3 on the plasma membrane. PIP3 binds to the signal proteins AKT
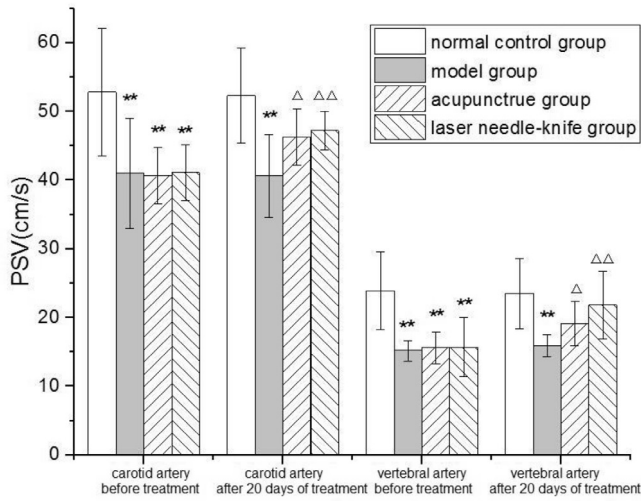
Fig. 2. PSV of right carotid artery and vertebral artery of rabbits in each group. Compared with normal control group, $*P < 0.05$, $**P < 0.01$; Compared with model group, $^{\triangle}P < 0.05$, $^{\triangle\triangle}P < 0.01$.
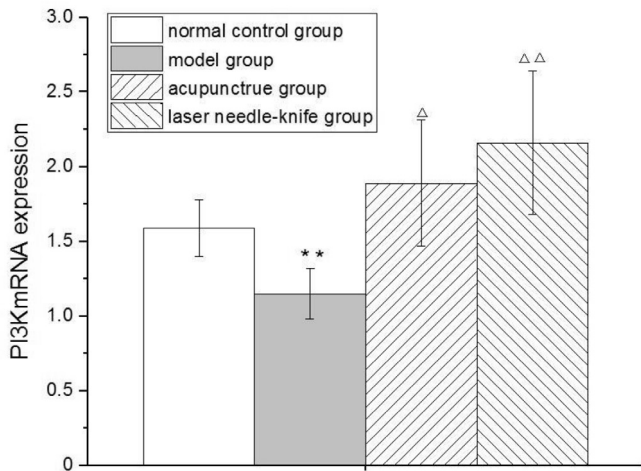

Fig. 4. AKT mRNA expression in right carotid artery of rabbits in each group. Compared with normal control group, $*P < 0.05$, $**P < 0.01$; Compared with model group, $^{\triangle}P < 0.05$, $^{\triangle\triangle}P < 0.01$.
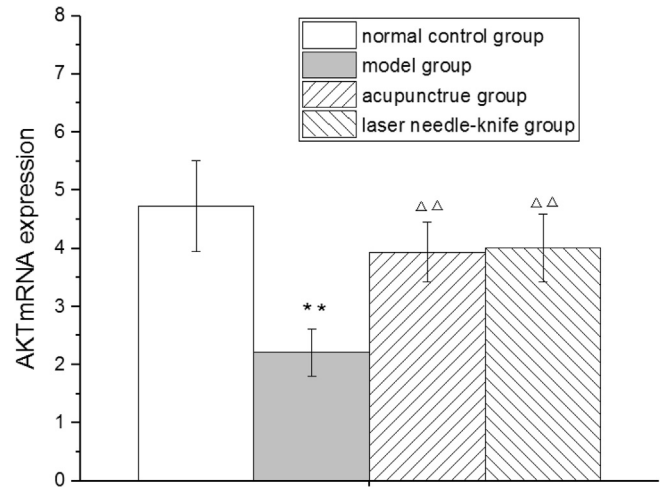

Fig. 3. PI-3K mRNA expression in right carotid artery of rabbits in each group. Compared with normal control group, $*P < 0.05$, $**P < 0.01$; Compared with model group, $^{\triangle}P < 0.05$, $^{\triangle\triangle}P < 0.01$.
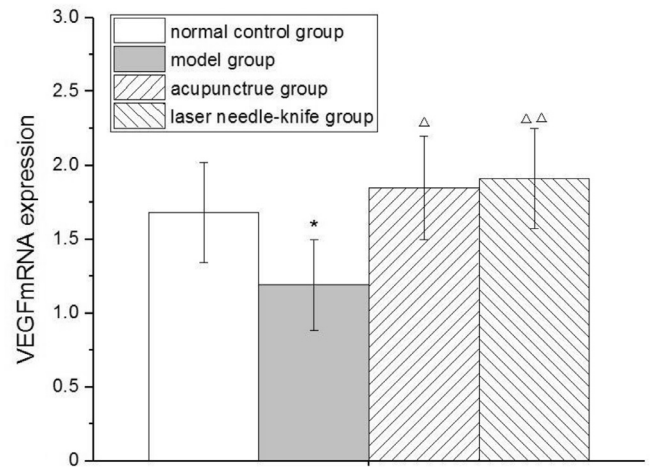

Fig. 5. VEGF mRNA expression in right carotid artery of rabbits in each group. Compared with normal control group, $*P < 0.05$, $**P < 0.01$; Compared with model group, $^{\triangle}P < 0.05$, $^{\triangle\triangle}P < 0.01$.

and PDK1 that contain the PH domain in the cell, causing Ser308 of PDK1 phosphorylated AKT protein to activate AKT, forming the PI-3K/Akt signaling pathway (Dar et al., 2018; Ma et al., 2018). AKT phosphorylates and inactivates nodular sclerosing factor 2, thus inducing the formation of active Rheb (Hsieh et al., 2014), and Rheb in turn phosphorylates and activates mammalian target of rapamycin (mTOR) (Peng et al., 2018), mTOR can directly enhance the transcriptional activity of hypoxia inducible factor-1α (HIF-1α), leading to its metastasis to the nucleus and activation with the structural subunit HIF-1β to form the HIF-1 heterodimer complex, and then in combination with a hypoxia response element in the HIF-1α target gene, the transcriptional activity of the target gene is regulated (Shen et al., 2017). The target function of HIF-1α-regulated target genes is to promote angiogenesis and increase local oxygen flux. VEGF is a heparin-binding growth factor that is specific for vascular endothelial cells and is the most important factor among the more than 30 angiogenesis-related factors identified so far. Under hypoxic conditions, VEFG can be induced by HIF for transcriptional activation (Wang et al., 2018), and its biological effects are mainly reflected in two aspects. (1) To promote the division and proliferation of vascular endothelial cells, thereby generating new blood vessels (Mehmood et al., 2018); (2) To increase microvascular permeability as a vascular permeability factor (Xu et al., 2018).

Researchers have found that the main mechanism of injecting allogeneic blood into rabbit modeling site is the meridian qi-circulation difficulty caused by blood stasis, resulting in dizziness; local occupation, tissue-like inflammatory lesions produced by allogeneic immune responses, muscular contracture, mechanical disequilibrium, vertigo produced by direct or indirect stimulation of vertebral artery and its surrounding sympathetic nerves. This model has become a classical CSA model based on traditional Chinese medicine blood theory and meridian theory. The CSA rabbit model was prepared following this method. It was found that after the model was established, the rabbits in the model group showed markedly decreased activity, unresponsiveness, bow and back curling, poor coat color, reduced water intake and food intake, thin sloppy stool, dark purple ears and tongue compared with the normal group. After the completion of modeling, compared with the blank group, the behavior of the rabbits in the model group was changed, and the blood flow velocity was significantly reduced, which was statistically different from that of the normal group, indicating that the CSA experimental model was successfully established.

Laser acupotomy is an improvement to traditional small needle knives. It is simple in equipment, simple in operation, effectively avoids trauma to the body, with a good therapeutic effect and no toxic or side effects. It is easy for patients to accept. As a novel technology, laser acupotomy is currently rarely used in CSA treatment, but related studies have shown that it has significant clinical efficacy in improving blood circulation and anti-inflammatory analgesia. Shao et al. (2014) found that the laser has an evoked effect on the regeneration of microvessels, and its principle is closely related to the activation of PI3K. Al Rashoud et al. (2014)used laser acupotomy to treat osteoarthritis of the knee. It is believed that laser acupotomy can promote capillary dilation and improve local blood circulation, increase pain threshold, achieve analgesic effect, and also have significant anti-inflammatory effect, thereby reducing patients' pain and improving the quality of life. Huang et al. (2014) used laser acupotomy to treat temporomandibular disorders (TMD), and also found that laser irradiation can relieve pain, relax muscles and promote blood circulation, and can regulate metabolism, change histopathological conditions and promote the recovery of tissue health, and it is safe and efficient without side effects. Laser acupotomy is essentially a process of energy conversion and transmission. After being absorbed by a certain photon, the tissue irradiated by laser light converts light energy into heat energy, which increases the local temperature, dilates blood vessels and promotes angiogenesis, and improves blood circulation, restores hemodynamic balance and promotes metabolism. Since the major cause of CSA is the decrease of local cerebral blood flow due to cone-basal artery insufficiency, laser acupotomy is theoretically particularly suitable for the treatment of CSA.

5. Conclusions

From the results of the phased study of this project, the main mechanism of laser acupotomy combination therapy in the treatment of CSA is to stimulate the generation of vertebral artery microvessels by the PI3K- AKT- VEGF signal path, thereby effectively improving the blood circulation of the vertebral artery, changing the abnormality of vertebral artery hemodynamics caused by CSA, and facilitating local blood supply. So it is the next work to find out how laser-needle knife affects PI3K mRNA gene expression signals transduction pathway in CSA rabbit and the difference between original and new capillary blood vessels.

Acknowledgments

References

Akin, S., Aksoy, D.Y., Akin, S., Kilic, M., Yetisir, F., Bayraktar, M., 2017. Prediction of central lymph node metastasis in patients with thyroid papillary microcarcinoma. Turkish J. Med. Sci. 47 (6), 1723–1727.

Al Rashoud, A.S., Abboud, R.J., Wang, W., et al., 2014. Efficacy of low-level laser therapy applied at acupuncture points in knee osteoarthritis: a randomised double-blind comparative trial. Physiotherapy 100 (3), 242–248.

Chen, Z.H., Huang, W.W., Tian, T.T., et al., 2018. Characterization and validation of potential therapeutic targets based on the molecular signature of patient-derived xenografts in gastric cancer. J. Hematol. Oncol. 11, 20.

Chin, H.K., Horng, C.T., Liu, Y.S., et al., 2018. Kaempferol inhibits angiogenic ability by targeting VEGF receptor-2 and downregulating the PI3K/AKT, MEK and ERK pathways in VEGF-stimulated human umbilical vein endothelial cells. Oncol. Rep. 39 (5), 2351–2357.

Choi, J.M., Hong, H.J., Chang, S.K., et al., 2014. Cervical spondylosis: a rare and curable cause of vertebrobasilar insufficiency. Eur. Spine J. 23 (2), S206–S213.

Dar, N.J., Satti, N.K., Dutt, P., et al., 2018. Attenuation of glutamate-induced excitotoxicity by withanolide-A in neuron-like cells: Role for PI3K/Akt/MAPK signaling pathway. Mol. Neurobiol. 55 (4), 2725–2739.

Deng, S.Z., Zhao, X.F., Huang, L.F., et al., 2015. The quantity-effect relationship and physiological mechanisms of different acupuncture manipulations on posterior circulation ischemia with vertigo: study protocol for a randomized controlled trial. Trials 16, 152.

Fu, H.B., Wang, C.M., Yang, D.J., et al., 2018. Curcumin regulates proliferation, autophagy, and apoptosis in gastric cancer cells by affecting PI3K and P53 signaling. J. Cell. Physiol. 233 (6), 4634–4642.

Hou, Z.Z., Xu, S.B., Li, Q.L., et al., 2017. The efficacy of acupuncture for the treatment of cervical vertigo: a systematic review and meta-analysis. Evid-Based Compl. Alt. 1–13, 7597363.

Hsieh, C.T., Chung, J.H., Yang, W.C., et al., 2014. Ceramide inhibits insulin-stimulated Akt phosphorylation through activation of Rheb/mTORC1/S6K signaling in skeletal muscle. Cell. Signal. 26 (7), 1400–1408.

Hu, X.M., Zheng, Z., Yang, S.T., et al., 2005. Establishment of a cervical spondylotic arteriopathy rabbits model by static blood blocking collaterals. J. Sichuan Tradit. Chin. Med. 23 (12), 19–22.

Huang, Y.F., Lin, J.C., Yang, H.W., et al., 2014. Clinical effectiveness of laser acupuncture in the treatment of temporomandibular joint disorder. J. Formos. Med. Assoc. 113 (8), 535–539.

Kevrekidis, D.P., Minarikova, D., Markos, A., Malovecka, I., Minarik, P., 2018. Community pharmacy customer segmentation based on factors influencing their selection of pharmacy and over-the-counter medicines. Saudi Pharm. J. 26 (1), 33–43.

Kim, M.S., 2018. C2 segmental-type vertebral artery diagnosed using computed tomographic angiography. J. Korean Neurosurg. Soc. 61 (2), 194–200.

Li, Z., Han, C., Wei, D., 2018. Empirical research on the relationship between natural gas consumption and economic growth in the northeast asia. Energy Environ. 29 (2), 216–231.

Liu, F., Wei, W., Yang, G.Y., et al., 2017. Therapeutic effects and finite element analysis of a combined treatment using laser needle-knife with supine repositioning massage on patients with cervical spondylotic vertebral arteriopathy. Int. J. Pattern Recogn. 31 (11), 1757008.

Liu, Z., Zhu, G.J., Getzenberg, R.H., et al., 2015. The upregulation of PI3K/Akt and MAP Kinase pathways is associated with resistance of microtubule-targeting drugs in prostate cancer. J. Cell Biochem. 116 (7), 1341–1349.

Ma, S.L., Chen, J.W., Chen, C., et al., 2018. Erythropoietin rescues memory impairment in a rat model of chronic cerebral hypoperfusion via the EPO-R/ JAK2/STAT5/PI3K /Akt/GSK-3 beta pathway. Mol. Neurobiol. 55 (4), 3290–3299.

Mao, L.Y., Chen, Q.Y., Gong, K., et al., 2018. Berberine decelerates glucose metabolism via suppression of mTOR-dependent HIF-1 alpha protein synthesis in colon cancer cells. Oncol. Rep. 39 (5), 2436–2442.

Markus, H.S., Larsson, S.C., Kuker, S.C., et al., 2018. Stenting for symptomatic vertebral artery stenosis: the vertebral artery ischaemia stenting trial. J. Vasc. Surg. 67 (3). 986–994.

Mehmood, K., Zhang, H., Li, K., et al., 2018. Effect of tetramethylpyrazine on tibial dyschondroplasia incidence, tibial angiogenesis, performance and characteristics via HIF-1 alpha/VEGF signaling pathway in chickens. Sci. Rep-UK 8, 2495.

Peng, H., Kasada, A., Ueno, M., et al., 2018. Distinct roles of Rheb and Raptor in activating mTOR complex 1 for the self-renewal of hematopoietic stem cells. Biochem. Bioph. Res. Co. 495 (1), 1129–1135.

Saranya, S., Vijayarani, K., Pavithra, S., 2017. Green synthesis of iron nanoparticles using aqueous extract of musa ornata flower sheath against pathogenic bacteria. Ind. J. Pharm. Sci. 79 (5), 688–694.

Shao, Y., Hang, L., Yu, H.T., et al., 2014. Inhibitory effects of naringenin and its complex of copper (II) with free ligand on formation of choroidal neovascularization in rats induced by laser. Int, Eye Sci. 14 (1), 23–27.

Shen, Y.M., Liu, Y.Y., Sun, T., et al., 2017. LincRNA-p21 knockdown enhances radiosensitivity of hypoxic tumor cells by reducing autophagy through HIF-1/ Akt/mTOR/P70S6K pathway. Exp. Cell Res. 358 (2), 188–198.

Wang, C.G., Lou, Y.T., Tong, M.J., et al., 2018. Asperosaponin VI promotes angiogenesis and accelerates wound healing in rats via up-regulating HIF-1 alpha/VEGF signaling. Acta Pharmacol. Sin. 39 (3), 393–404.

Wen, Y., Zhang, C., Zhao, X.F., et al., 2016. Safety of different acupuncture manipulations for posterior circulation ischemia with vertigo. Neural. Regen. Res. 11 (8), 1267–1273.

Xu, J., Sun, Y.X., Wu, T.Y., et al., 2018. Enhancement of bone regeneration with the accordion technique via HIF-1/VEGF activation in a rat distraction osteogenesis model. J. Tissue Eng. Regen. Med. 12 (1), E1268–E1276.

Zhu, S.W., Yang, Y., Liu, Y.G., et al., 2018. Anatomical features and clinical significance of radiculomuscular artery variants involving the suboccipital segment of vertebral artery angiographic and cadaver studies. Clin. Neuroradiol. 28 (1), 75–80.

Further reading

Li, X.H., Liu, M.H., Zhang, Y., et al., 2017. Acupuncture for vertebrobasilar insufficiency vertigo: protocol for a systematic review and meta-analysis. Medicine 96, (50) e9261.